Diffraction-Enhanced Imaging

Zhong Zhong
National Synchrotron Light Source
Brookhaven National Laboratory
zhong@bnl.gov

INTRODUCTION

Despite recent advancements in mammography, MRI, and CT, challenges remain. The rate of false negative in mammography is still about 10%; cartilage is difficult to visualize by radiological means; and the contrast of chest x-ray is too low to detect early stages of emphysema and edema. DEI (Diffraction Enhanced Imaging) is a novel radiography method that introduces fine selectivity for the angular deviation of x-rays traversing the subject. It uses collimated x-ray beams produced by a perfect crystal monochromator and an analyzer crystal positioned between the subject and the detector. DEI's angular sensitivity allows measuring, besides the x-ray attenuation of the subject, the gradient of x-ray index of refraction, and the yield of "ultra-small-angle scattering". Since DEI's contrast mechanism does not rely on the absorption of the subject, it is ideally suited for soft-tissue imaging.

Since the invention of DEI in 1995, attempts have been made to investigate the applicability of DEI to breast imaging and other areas of radiology of clinical relevance. Preliminary studies with human breast cancer and human ankle cartilage specimens, as well as in vivo animal imaging show that a) the "index of refraction image" highlights boundaries between different tissue types (including breast tissue and tumor), b) the breast images provide information on lesion border detail and associated features that are not detected by conventional imaging, c) lungs were substantially highlighted in the "apparent absorption" image, and d) DEI differentiates between normal and damaged human excised talus cartilage.

Ongoing Studies at X15A systematically investigate the applicability of DEI to clinical imaging, by concentrating on three areas of soft-tissue imaging: breast, lung imaging and cartilage imaging. To be of general benefit, a clinical system should eventually be developed. The feasibility study and optimized parameters obtained by the present study, along with flux calculations and measurements from conventional based sources with appropriate x-ray optics, will allow assessment of the viability of a laboratory-based DEI system.

PRINCIPLES OF DEI

Conventional radiography uses an area beam which, after traversing and interacting with the subject, is intercepted and recorded by an area detector. The interaction of x-rays with the subject is complex, involving absorption, refraction and scattering. The scattering may include small angle scattering (scattering angles less than milliradians) and x-ray refractionwhich carries information about the subject's structure on the length scale up to microns. This information is lost in normal radiography because of its small angle nature.

X-ray diffraction from perfect crystals, whose narrow reflection angular width (on the order of a few microradians) and peak reflectivity of close to unity, provides the tools necessary to prepare and analyze x-ray beams traversing an object on the microradian scale. In DEI an imaging beam is prepared by diffracting the polychromatic beam from the synchrotron to create a nearly mono-energetic imaging beam. This beam is then passed through the object being imaged as in conventional radiography. However, a matching crystal is placed between the object and the detector. This crystal is set at or near the peak of Bragg diffraction and is called the analyzer crystal. A schematic representation of a synchrotron radiography and DEI system is shown in **Figure 1**.
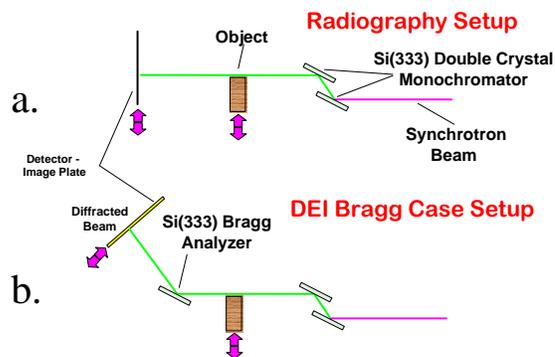
Figure 1. *Experimental Setup. Figure 1a schematically shows the synchrotron setup used to obtain radiographs of the object. Figure 1b shows the addition of the analyzer crystal (Bragg or reflection geometry) used to implement the DEI system.*

The range of angles which can be accepted by the analyzer is a few microradians, therefore, the analyzer provides scatter-rejection at the microradian level which is below the capabilities of conventional anti-scatter techniques such as slit collimation and grids. The scatter rejected falls into a category referred to as small angle scattering. Small angle scattering arises from diffraction from organized structures with dimensions up to micron sizes. This scattering intensity which would normally appear in the image is missing and appears in the same way as absorption in the image. This scatter rejection contrast is called extinction contrast, drawing from a similar term used in optics and x-ray diffraction to describe intensity loss due to diffraction and scattering. Therefore, in DEI, the image which represents the absorption of the object by x-rays is referred to as the apparent absorption image since it has contrast derived from both absorption and scatter rejection, or extinction.

The analyzer rocking curve shape will introduce a sensitivity to refraction occurring within the object when the analyzer is de-tuned from the peak position. Density, thickness and/or material variations in an object will refract the x-rays as they cross through the material. These small angular variations are generally in the sub-microradian range. The steep sides of the reflectivity curve converts these subtle angle variations into intensity variations, thus making refraction effects visible in an image. We have shown that by acquiring an image pair with the analyzer set to diffract on each side of the rocking curve, we can separate refraction effects from combined absorption and extinction effects.

Thus with the DEI technique we have introduced two new sources of image contrast to radiography, refraction and extinction. Each of these new image contrast sources may be further developed to apply to medical and biological imaging.

INSTRUMENTATION

The experimental setup used to apply this technique is shown in **Figure 1**, which shows both the synchrotron radiography system (**Figure 1a**) and the addition of the analyzer crystal for the DEI system (**Figure 1b**). The white synchrotron beam is made nearly monochromatic by a silicon double crystal monochromator. The beam energy is adjustable between 12 and 50keV.

Since January 1998, a half-time dedicated DEI facility was established at the NSLS X15A beamline. X15A is a standard NSLS bending-magnet beamline. **Figure 2** shows the setup of DEI at X15A. The monochromator and analyzer are both positioned on a granite block which is 0.375 meter wide, 0.3 meter tall, and 2.1 meters long. The granite block is isolated from the floor's vibration by three stacked layers of rubber (each 10 mm thick) placed under the table holding the block.

The monochromator tank is mechanically isolated from the beamline pipe by a 2 cm air-gap. The ozone generated by x rays passing through this air gap is reduced to an insignificant level by a 1-mm-thick aluminum filter placed downstream of the beamline's Be window. The section between the Be window and aluminum filter is also protected from ozone by a helium flow.

The sample's scanning stage and shutter is placed on a platform that is mechanically isolated from the granite block by supporting the platform directly from the floor. Since the incident beam is polychromatic, non-dispersive crystals for both the monochromator and analyzer make use of the full beam height. The flux of the monochromatic beam on the sample is determined by the integrated reflectivity of the two-crystal monochromator.

The imaging beam was approximately 130 mm wide and 2 mm high at the location of the object. An ionization chamber was used to measure the radiation exposure at the surface of the object. The specimen to be imaged is mounted on a scanning stage that is driven by a stepping motor. The x-ray beam transmitted through the object can be either imaged directly as in normal radiography or following diffraction in the vertical plane by the silicon crystal analyzer. Radiation exposure to the image plate is controlled by adjusting the scan speed and absorbers in the incident beam.
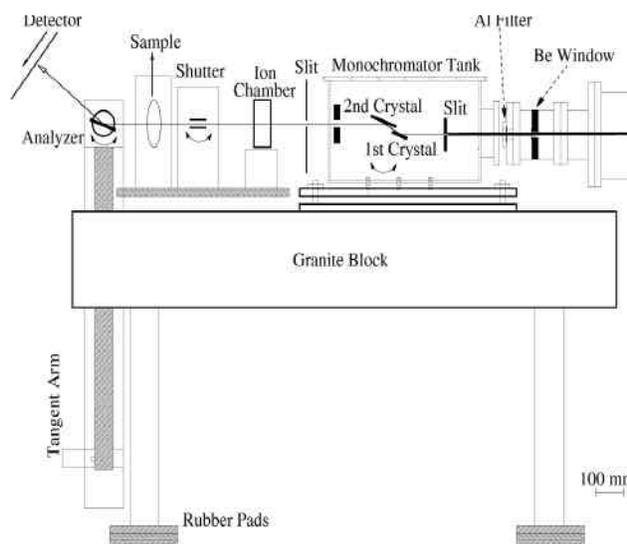
Figure 2. Setup at the NSLS X15A beamline.

Typical scanning times are 4 to 200 seconds. These limits are dictated by the scanning motors and the desired radiation dose.

Monochromator

The ideal monochromator for DEI would be a channel-cut device, but due to the extreme width (130 mm) required for the images, it is difficult to fabricate. Instead, an alternative to a channel-cut system is used. The monochromator consists of two parallel Bragg crystals. The crystals are perfect float zone silicon with the surface parallel to the [111] planes. Thus, each crystal can be used in the symmetric Bragg mode with [nnn] diffraction (n can be 1, 3, 4, 5, etc.) depending on the angular resolution desired.

The monochromator is a box-type design with a fixed offset of 1 cm between the two crystals. The first and second crystals are mounted on the bottom and top plates of the box, respectively. Each crystal is fixed to a kinematic mount allowing the Bragg angle and azimuthal angle to be adjusted. The box is mounted on a cradle so that the middle of the first crystal's surface is at the center of rotation to accommodate changes in the beam's energy. The resolution of the cradle is 2.5X10^{-4} degrees. The top plate of the box can slide along the direction of the incident beam in 12.7 mm steps to change the distance between the two crystals.

This simple box-type design is particularly resistant to vibration. Due to this mechanical stability, with the crystals diffracting in the [333] mode at 18 keV, the intensity modulation of the monochromatic beam is less than 1% peak-to-peak. The monochromator assembly is placed inside a stainless-steel tank into which helium at atmospheric pressure flows to prevent corrosion caused by ozone. Both the incident and exit windows of the tank are made of 100-micron-thick Kapton. The tank has a flange to accommodate supply lines for electricity, water and helium.

Each crystal is 10 mm thick and 150 mm wide with strain-relief cuts (2 mm wide and 8 mm deep) on the top at 10 mm from its ends. Thus, the useful width (perpendicular to the beam) of the crystal is 128 mm. The first crystal is 60 mm long and the second is 90 mm long. The length of the second crystal allows for a long range of change in energy without the need to adjust the distance between the two crystals. For example, in the [333] mode, if the second crystal is centered to diffract 40 keV (the distance between the center of the two crystals being 66.5 mm), the monochromator's energy can be changed from 15 keV to 65 keV by adjusting the angle of the box with the cradle without sliding the second crystal.

The second crystal's Bragg angle and azimuthal angle can be adjusted by three piezo-driven screws (New Focus Picomotor 8303). The resolution of the Picomotor is less than 0.03 microns, so the second crystal can be finely adjusted to lie parallel to the first crystal.

Analyzer

The analyzer crystal is the same as the second crystal of the monochromator (150 mm wide by 90 mm long with similar strain relief cuts). The crystal's Bragg angle is controlled by a 1 meter long tangent arm. The tangent arm is driven by a linear translator with 0.1 micrometer resolution, providing an angular resolution of 0.1 micro-radians. This resolution is sufficiently accurate to position the analyzer at any location on the analyzer's rocking curve, which has a full width at half maximum (FWHM) on the order of 1 micro-radians. The tangent arm is mounted on the same optical table or granite block as the monochromator. The analyzer is attached to the tangent arm by a motorized kinematic mount which adjusts the azimuthal angle of the analyzer crystal.

Detector

Images are acquired by scanning the sample vertically through the horizontal fan beam. Although a line-detector would be optimum for the present line-scan system, it is currently not commercially available. Most of our experiments were carried out with image plate readers (Fuji Medical Systems, model BAS2500). Since the Bragg analyzer inverts the beam like a mirror, the image plate is scanned in the direction opposite to the sample's scan direction to avoid blurring the images. The image-plate scanner also is tilted to an angle of twice the Bragg angle from the vertical direction, so that the image plate is perpendicular to the beam diffracted by the analyzer. This configuration avoided blurring of the image due to the beam's height and the tilting of the diffracted beam. The pixel size of the images is 50 micron by 50 micron.

TYPES OF MEASUREMENT

Typically, several types of measurements were taken to investigate various aspects of the sample and DEI effects. For a normal radiograph, the image plate is placed behind the sample without the analyzer crystal and the sample and image plate scanned vertically together at the same speed. This is comparable to conventional digital x-ray radiograph and was taken for

comparison with the DEI images.

For a DEI scan, the analyzer is fixed at a specific angle and the sample and the image plate scanned at the same speed in opposite directions.

A multi-scan is a series of DEI scans, each differing in the angle of the analyzer at which the image is acquired. Multi-scan images are spatially separated on the image plate by translating the image plate appropriately in-between scans. In this way, images of the same sample at different analyzer positions can be acquired using the same plate. Since most images are less than 100 mm by 100 mm, the multi-scan mode efficiently uses the image-plate's area (200 mm by 250 mm) and reduces the time spent reading the plates.

Another technique to study the response of a feature in a sample is a rocking-curve scan. In this type of scan, the region of interest on the sample is moved into the beam and a series of fixed-time exposures are
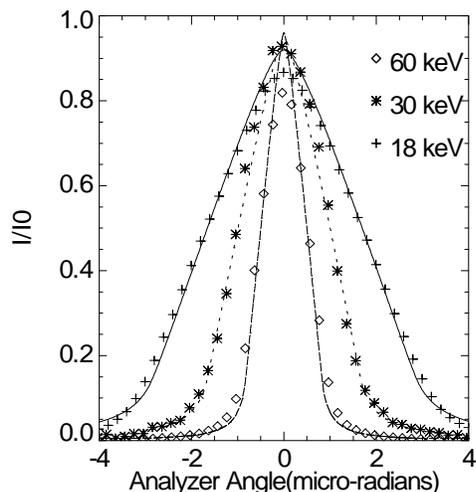
Figure 3. *Measured rocking curves at 18, 30 and 60 keV.*

taken at incremental analyzer angles. The image plate's position is regularly increased vertically so that different exposures are separated on the image plate. As a result, a vertical profile on the image plate represents a rocking curve of the analyzer through a point on the sample. Rocking-curve scans can reveal extinction contrast easily, and represent a spatially-resolved measurement of the small-angle scattering by the sample.

All scans are controlled by a PC running a Windows-based C program. The program was specifically written to control the DEI experiment. The program obtains from the user the type of scan, scan range and analyzer positions, and performs the scan by controlling the image-plate's motion (both horizontal and vertical), the sample's motion and the analyzer's position

through stepper motors. The program also monitors the ion-chamber's response throughout the scan to obtain dose information and controls the shutter.

DATA ANALYSIS

The beamline computer has an IDL license, and can be used for analyzing data. All source codes for display, registering, and analyzing the images acquired are available to users who wish to undertake image analysis at their own computer.

EXAMPLES

Characterization of DEI's Sensitivity

The rocking curve of the analyzer crystal characterizes the angular sensitivity of a DEI system. The rocking curve is the convolution of the analyzer's reflectivity curve and the angular distribution of the beam generated by the monochromator. **Figure 3** shows the rocking curves measured at 18-, 30-, and 60-keV. The solid lines show the theoretical rocking curves.

The crystal reflection affects the structure-factor of the reflection and thus the width of the analyzer rocking curve. A higher order reflection index gives a narrower the rocking curve width, thus producing more pronounced DEI contrast. All the preliminary experiments were done with either (111) or (333) reflections, with the (333) reflection yielding far better results than the (111) reflection, thus promising even better images with the (555) or higher reflection. Attempts to perform DEI at (555) were made and have resulted in a novel x-ray optics concept of using x-ray refraction of harmonic selection (Zhong 2000), paving a clear path to actually use the (555) reflection.

For more information, see: Z. Zhong, *J. Appl. Cryst.* **33** (2000) 1082-1087, and , Z. Zhong, W. Thomlinson, D. Chapman and D. Sayers, *Nucl. Instrum. Meth. in Phys. Res. A.* **450** (2000) 556-567.

Implementation of DEI in the CT Mode

DEI CT of an acrylic phantom with tilted channels (filled with oil) were reconstructed, resulting in a separation of the refraction image from the absorption image (**Figure 4**). The image contrast of the refraction image was proportional to the gradient of the refractive index. There was a remarkable agreement between the linearity trends of the experimental findings and the theoretical index-of-refraction predictions.

From our study we draw the following conclusions:
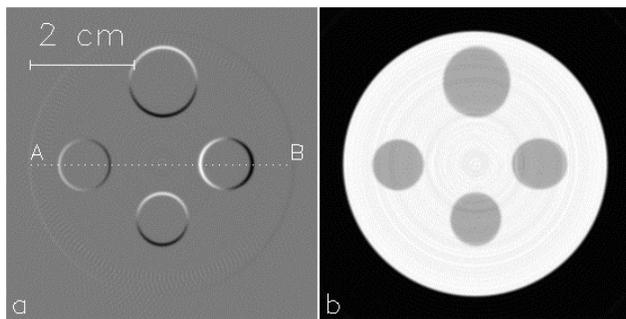
Figure 4. *Images of the slanted-channel phantom obtained at 22 keV with 333 monochromator and analyzer: a) refraction image, and b) apparent-absorption image.*

a) DEI CT projections are complete sets, and thus can be reconstructed conventionally, b) the separation of the refraction image from the other image components is complete for material with little small-angle scattering, such as oil and acrylic, c) the image contrast is proportional to the gradient of the refractive index, and, d) there is a remarkable agreement between the linearity trends of the experimental findings and the theoretical index-of-refraction results.

For more information, see: A. Dilmanian, Z. Zhong, B. Ren, X. Y. Wu, et. al., "Computed Tomography of X-ray Index of Refraction Using the Diffraction Enhanced Imaging Method", *Phys. Med. Bio*. **45** (2000) 933-946.

Breast Imaging

Mammographic technology has improved dramatically in the last two decades. These improvements include the development of dedicated mammography equipment with appropriate x-ray beam quality, adequate breast compression and automatic exposure control. Digital mammography is the most recent development and is just now being introduced into the clinic and holds promise of improved early detection of breast cancer. However, all these currently existing systems depend on the depiction of x-ray absorption to define the differences between normal and abnormal tissues. The new radiographic imaging method, Diffraction Enhanced Imaging, DEI, partly depends upon the refractive properties of an object in the creation of a scatter-free image. This new method, which seeks to improve the x-ray beam properties for improved contrast, along with the

new digital mammography detectors could improve early detection of occult disease.

Seven breast cancer specimens were examined with DEI at 18 keV and 30 keV with a silicon crystal analyzer using 333 reflection. The specimens were formalin-fixed human breast cancer specimens, including three infiltrative lobular and four infiltrating ductal carcinomas. These specimens were approximately 1 cm thick. Each biologic sample was sealed in a plastic bag and compressed between two Lucite plates so that the absorbing thickness was approximately 40 mm. For each sample, five DEI images were obtained at analyzer angular positions of 0 (peak position), W/2, and W on the rocking curve, where W is the full-width at half maximum of the rocking curve. Images of the same specimen were also obtained with use of a digital mammographic unit (SenoScan, Fischer Medical Imaging, Boulder, Colo.).

DEI and digital radiographs of the specimens were subsequently evaluated by one experienced breast imager, who identified regions of interest within the diffraction-enhanced images that showed apparently increased lesion information, for example, areas of in-
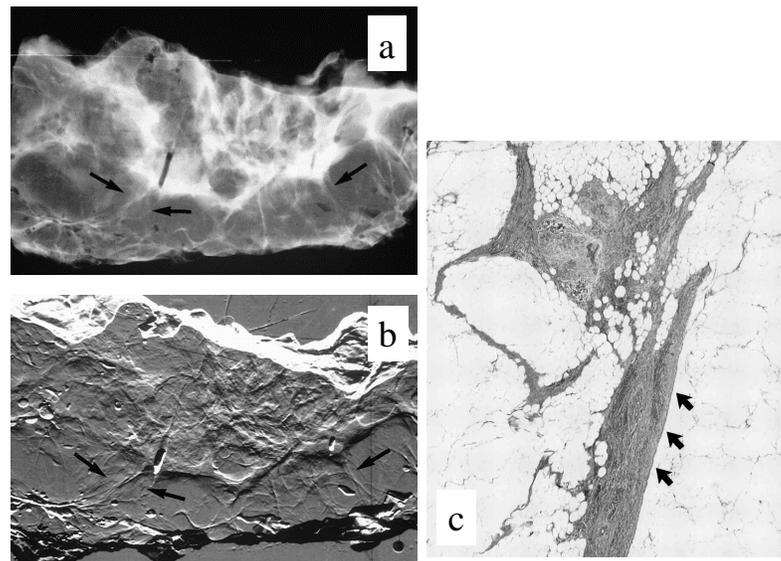
Figure 5. *Specimen with invasive lobular carcinoma, which typically grows in single files of cells.* **(a)** *Digital radiograph of the specimen. Note the vague linear densities along the inferior margin of the lesion, some of which are marked with arrows. A scratch artifact lies across the top portion of the image.* **(b)** *Diffraction-enhanced image of the same specimen. Note the increased prominence and number of lines that extend from the inferior border of the lesion at the arrows.* **(c)** *Photomicrograph of the spiculations identified between the two arrows on the left in* **b** *shows a band of fibrous tissue with invasive lobular carcinoma (arrows). The other spiculations identified by the single arrow on the right in* **b** *proved to be both infiltrating lobular carcinoma and fibrous bands. (Hematoxylin-eosin stain; original magnification, x10.)*

creased surface spiculation. DEI Images were compared with digital radiographs of the specimen, and regions of increased detail were identified. Histologic whole-mount slides of the specimens were made. Six of the seven cases (86%) showed enhanced visibility of surface spiculation that correlated with histopathologic information, including extension of tumor into surrounding tissue.

As an example of DEI's improved depiction of spiculations corresponding with tumor extension, Fig.5 shows images of a breast tissue with invasive lobular carcinoma that extends to the edge. Improved detail has been confirmed as representing real histologic-anatomic structures. For example, spiculations that are better visualized with the DEI method correlated with structures seen on the histologic slides by the pathologist, sometimes representing breast cancer itself extending into the surrounding breast tissue, and sometimes representing fibrosis (scarring), the breast's natural reaction to the tumor's presence. **Figure 5** also shows the improved visualization of spiculations representing tumor extension, spiculations representing fibrosis, and calcifications seen within the DEI image that were visualized within the pathologic specimens but that could not be seen on the conventional radiographs. Clearly, this amount of improved detail is quite promising, especially when one considers the fact that we have not yet optimized this technique for breast imaging.

Overall, the DEI images have shown improved visualization of calcifications (in 6/7 cases) and spiculations (or architectural distortion) (in 7/7 cases). Calcifications and spiculations are mammographic features that aid radiologists in detection and classification of breast lesions. In no instance has the increased lesion detail present in the DEI images proven to be artifactual.

For more information, see: E. D. Pisano, R. E. Johnston, D. Chapman, J. Geradts, et. al., *Radiology*, **214** (2000) 895-901.

Cartilage Imaging

Because of its high water content, cartilage can not be visualized with conventional radiography. Therefore, cartilage destruction is only identified with x-rays through narrowing of the space between the bony sur-

faces of the joint that is normally occupied by healthy articular cartilage. As the cartilage is destroyed the joint space narrows – obviously a point at which the degeneration of cartilage has reached serious consequences. A high-resolution radiographic method to directly visulize the defects in cartilage is thus highly-desirable.

DEI has been applied to image human articular cartilage from the distal part (talus) of the ankle (talocrural) joint that are either macroscopically normal or display damages typical of early degenerative stages. None of the 12 donors used in this study has a known history of osteoarthritic disease. For the normal ankles (n=4), the ages were 34 to 54 years, and for the damaged ankles (n=8) the ages were 51 to 66 years. The tali were x-rayed in a posterior-to-anterior direction.
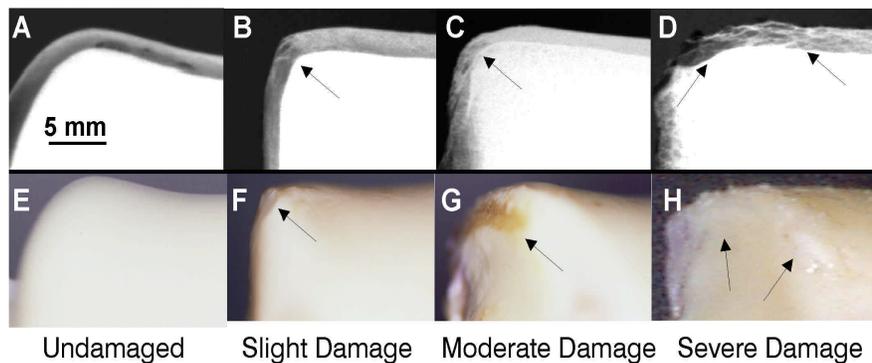
Figure 6. Sections of DEI from the talar dome of the ankle joint. DEI images of normal and damaged articular cartilage from the talus of human ankles at 30 keV (top row) are shown with the corresponding macroscopic pictures (bottom row). The DEI cartilage tissue image of the intact talus (a, e) shows a homogenous and moderately dense structure. In the damaged tali (b-d, f-h) the degenerative sites (arrows) are clearly detected by distinctive structural heterogeneities within the cartilage. The arrows indicate particular sites of lesions.

Figure 6 shows examples of a normal and several damaged tali with the corresponding DEI images. The images were acquired at 18 keV with [333] reflection. The DEI images taken with the analyzer at the peak of the rocking curve were shown. The cartilage tissue can clearly be detected and distinguished from the bone. The structure of cartilage on the normal talus looks homogenous, with an average height of 1.5 mm and moderate density (**Figure 6A**). This pattern changes in damaged cartilage, the tissue is no longer homogenous but shows patterns that suggest structural alterations (**Figure 6 B-D**) and that correspond with the sites of macroscopic damage (**Figure 6F-H**). At higher magnification of certain areas, distinct structural alterations can be seen. Of special interest are the thin white
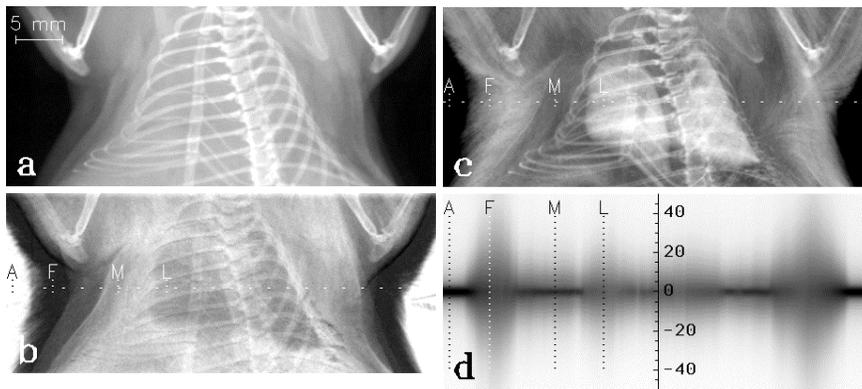
Figure 7. *a) Normal radiograph of a mouse at 18 keV. Darker color represents greater x-ray intensity. b), c) DEI images with the analyzer at -10, and 0 micro-radians, respectively. Refer to text for explanations of A, F, M and L regions. d) Rocking curve scan through the middle of the lung, indicated by the horizontal dashed lines in the images above; Vertical axis corresponds to changing analyzer angle from -50 micro-radians to 50 micro-radians.*

lines on a dark background (arrows in **Figure 6B-D**). It is possible that those white lines represent certain structural changes which give rise to specific refraction patterns or extinction effects detected by the imaging system. This would most likely develop at the edges of cartilage fibrillations, fissures or defects.

The preliminary study shows that it is possible to visualize articular cartilage using DEI. Moreover, the combination of the high spatial resolution that can be achieved with x-rays, and the independent detection of refraction patterns, scatter rejection and x-ray absorption make DEI capable of detecting not only articular cartilage and gross cartilage defects but also structural abnormalities within the tissue. DEI appears to be able to detect cartilage degeneration even in early stages, i.e. before any clinical evidence of disease evolves.

For more information, see: J. Mollenhauer, M. Aurich, Z. Zhong, C. Muehleman, et. al., "Diffraction Enhanced X-ray Imaging of Articular Cartilage", *J. Osteoarthritis and Cartilage*, **10** (2002) 163-171.

Lung Imaging

An *in vitro* mouse was studied at NSLS X15A using the silicon [333] monochromator and analyzer at 18 keV (Zhong *et al* 2000). **Figure 7a** is a normal radiograph of the thoracic region (around 20 mm thick) of the mouse taken at 18 keV. **Figures 7b** and **7c** are DEI images of the same region with the analyzer at -10 and 0 micro-radians, respectively.

Rocking curves through a line on the phantom were obtained by fixing the phantom in the fan beam and performing a series of exposures by incrementally changing the analyzer position and image plate verti-

cal position. The rocking curve is useful for quickly visualizing the optimum analyzer position for contrast enhancement of the desired features. A rocking curve scan was performed with the beam across the lung of the mouse, indicated by the horizontal dashed lines in **Figures 7b** and **7c**. **Figure 7d** shows the rocking curve scan; vertical direction corresponds to changing angle of the analyzer (from -50 micro-radians to 50 micro-radians), and the horizontal direction corresponds to the position across the animal's body.

Figure 8 plots the rocking curves of the analyzer with the beam through specific regions of interest A, F, M, and L. The position of A, F, M, and L in the images of the mouse and rocking curve scan are indicated in **Figures 7b, c, and d**. Curve A is the analyzer's rocking curve with the beam passing outside the mouse, through the air. F is the rocking curve through the fur on the mouse's side (only fur is present). M corresponds to a typical region of the body, including the animal's two thin layers of fur in front and back, and other body tissues, such as muscles and fat. The rocking curve through the lung region is represented by L. To account for the absorption of x-rays, the rocking curves were normalized so that the area under each
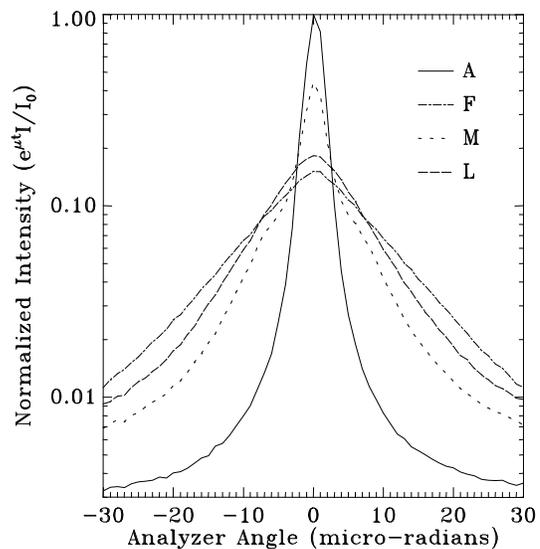
Figure 8. *Normalized analyzer rocking curves through the air (A), fur (F), lung (L), and muscle (M) regions.*

rocking curve is equal to the integrated reflectivity of the analyzer(area under the theoretical analyzer reflectivity curve).

The peak values of the normalized rocking curves in **Figure 8** are the amount of extra contrast due to DEI's rejection of scatter in images taken with the analyzer on top of the rocking curve. The values are 0.44, 0.18, and 0.15 for M, L, and F, respectively. And the corresponding normal absorptions obtained from **Figure 7a** are 0.61, 0.48, and 0.99. Due to the extinction contrast, the fur and lung appear very absorbing (more so than the bones) in a DEI image with the analyzer on the peak of the rocking curve. The extinction contrast is sensitive to the sub-microscopic structure of the object. Extinction contrast is also observed for lung (L), which has negligible absorption in normal radiograph, but is distinctly different from the other tissues of the body in extinction contrast.

DEI implemented in the CT mode at the NSLS using the 21-33 keV x rays also indicated that the extinction contrast in the lungs of the rat and mouse is many times larger than that in conventional radiography, exceeding that of soft tissue.

For more information, see: Z. Zhong, W. Thomlinson, D. Chapman and D. Sayers, *Nucl. Instrum. Meth. in Phys. Res. A.* **450** (2000) 556-567.

REPRESENTATIVE PUBLICATIONS

J. Mollenhauer, M. Aurich, Z. Zhong, C. Muehleman, A. A. Cole, M. Hasnah, O. Olturu, K. E. Kuettner, A. Margulis and L. D. Chapman, "Diffraction Enhanced X-ray Imaging of Articular Cartilage", *J. Osteoarthritis and Cartilage,* **10** (2002) 163-171.

Z. Zhong, "Using a Prism to Reject or Select Harmonic Reflections in an X-ray Monochromator", *J. Appl. Cryst.* **33** (2000) 1082-1087.

Z. Zhong, W. Thomlinson, D. Chapman and D. Sayers, "Implementation of Diffraction Enhanced Imaging Experiments: at the NSLS and APS", *Nucl. Instrum. Meth. in Phys. Res. A.* **450** (2000) 556-567.

E. D. Pisano, R. E. Johnston, D. Chapman, J. Geradts, M. V. Iacocca, C. A. Livasy, D. B. Washburn, D. E. Sayers, Z. Zhong, M. Z. Kiss, W. Thomlinson, "Human Breast Cancer Specimens: Diffraction Enhanced Imaging with Histologic Correlation - Improved Conspicuity of Lesion Detail Compared with Digital Radiography, *Radiology*, **214** (2000) 895-901.

A. Dilmanian, Z. Zhong, B. Ren, X. Y. Wu, L. D. Chapman, I. Orion and W. C. Thomlinson, "Computed Tomography of X-ray Index of Refraction Using the Diffraction Enhanced Imaging Method", *Phys. Med. Bio*. **45** (2000) 933-946.

D. Chapman, E. Pisano, W. Thomlinson, Z. Zhong, R. E. Johnston, D. Washburn and D. Sayers, "Medical and Biological Applications of Diffraction Enhanced Imaging". *Breast Disease.* **10** (3,4) (1998) 197-207.

D. Chapman, W. Thomlinson, Z. Zhong, R. E. Johnston, E. Pisano, D. Washburn and D. Sayers. "Diffraction Enhanced Imaging Applied to Materials Science and Medicine". *Sync. Rad. News*, **11.2** (1998) 4-11.

D. Chapman, W. Thomlinson, R. E. Johnston, D. Washburn, E. Pisano, N. Gmür, Z. Zhong, R. Menk, F. Arfelli, and D. Sayers, "Diffraction Enhanced X-ray Imaging". *Phys. Med. Biol*., **42 (**1997) 2015-2025.